C. R. Physique 18 (2017) 125–136

Contents lists available at ScienceDirect

Comptes Rendus Physique

www.sciencedirect.com

Energy and radiosciences / Énergie et radiosciences

Performance of low-power RFID tags based on modulated backscattering

Performance des tags RFID de faible puissance fondés sur la modulation d'un signal rétrodiffusé

Zeinab Mhanna *, Alain Sibille, Richard Contreras

LTCI, CNRS, Télécom ParisTech, Université Paris-Saclay, 46, rue Barrault, 75013 Paris, France

ARTICLE INFO

Article history:
Available online 13 December 2016

Keywords:
Radiocommunication
Low power
Ultra wideband
RFID tag

Mots-clés :
Radiocommunication
Faible puissance
Ultra large bande
Étiquette RFID

ABSTRACT

Ultra Wideband (UWB) modulated backscattering (MBS) passive Radio-Frequency IDentification (RFID) systems provide a promising solution to overcome many limitations of current narrowband RFID devices. This work addresses the performance of such systems from the point of view of the radio channel between the readers and the tags. Such systems will likely combine several readers, in order to provide both the detection and localization of tags operating in MBS. Two successive measurements campaigns have been carried out in an indoor reference scenario environment. The first is intended to verify the methods and serves as a way to validate the RFID backscattering measurement setup. The second represents a real use case for RFID application and allows one to quantitatively analyze the path loss of the backscattering propagation channel.

RÉSUMÉ

Les systèmes RFID ultra large bande (ULB) opérant en rétrodiffusion offrent une solution prometteuse pour surmonter de nombreuses limites des systèmes RFID conventionnels à bande étroite. Ce travail porte sur la performance des tels systèmes du point de vue de la propagation entre les lecteurs et les tags. Ces systèmes consistent à disposer plusieurs lecteurs afin de permettre à la fois la détection et la localisation des tags passifs opérant en rétrodiffusion. Deux campagnes de mesure successives ont été réalisées dans un environnement intérieur considéré comme scénario de référence. La première campagne de mesure est destinée à vérifier les principes et méthodes de base et sert de moyen de calibration du dispositif de mesure. La seconde configuration représente un cas d'utilisation pour l'application de la technologie RFID et permet d'analyser quantitativement l'atténuation du canal de propagation opérant en rétrodiffusion.

* Corresponding author.
E-mail address: zeinab.mhanna@gmail.com (Z. Mhanna).

http://dx.doi.org/10.1016/j.crhy.2016.11.008

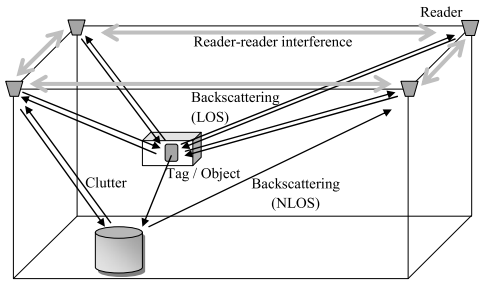

Fig. 1. System of tags and readers.

1. Introduction

This work takes place in the context of real-time localization systems (RTLS) made of a system of RFID tags and a set of readers. Although some systems have already existed for several years, the double challenge of a low consumption for the tags (ideally fully passive, i.e. without any local source of energy) and of a high spatial resolution for the localization capability is very hard to achieve. An approach has been pursued within a few years, which consists of a system of four readers at the corners of a parallelepiped (Fig. 1), and of tags operating according to a UWB modulated backscattering principle [1]. The benefit lies in the low-energy requirement within the tag, since for responding to the interrogation signal, it only needs to modify the impedance seen by the antenna port, according to a certain digital code. This process does not require an RF transmitter in the tag, with the associated energy consumption. The energy necessary for tag-reader communication is harvested from the reader's signal. At the reader, the modulated backscattered signal is received and can be detected by making use of the processing gain provided by the code. An extra code can be used by the reader itself, so to discriminate between its own backscattered signals from those coming from the other readers. In other words, among the system parameters that require careful design in order to control the link budget and the effect of interference, the coding strategy is essential [1]. Although some local energy source remains necessary, it can be much smaller than for an active transmitter and making use of a very small battery. Technologies are currently developed in order to cope with such needs, e.g., with supercapacitors [2].

The backscattering (BS) characteristics of UWB antennas for RFID systems indeed have been presented in several papers [3–5]. The UWB channel has also been widely studied, see, e.g., [6]. However, the UWB BS passive RFID channel has been poorly investigated in realistic scenarios. In this work, we address the system performance from the point of view of the radio channel between the readers and the tags. Typically, the backscattered signal is similar to that of a radar, meaning that it decays as the 4th power with the distance, which is extremely fast. In addition, since the technology is ultra wide band, the power spectral density is severely limited (typically well below 1 mW) and is much smaller than the power limitation for UHF RFID readers (typically 2 W). These facts are highly constraining in terms of detection range. However, since not only the propagation but also the antennas are involved in the link budget, it is possible to play with antenna characteristics in order to improve it somewhat.

In this paper, we concentrate on attenuation measurements between reader antennas and tags, which depend on the reader antenna characteristics and the tag antenna characteristics, including the polarization. We show that, by appropriately tuning the reader antenna characteristics, the 4th power distance dependence can be reduced, hence providing an enhanced detection range. It is also shown that, by considering multistatic scattering based on both monostatic and bistatic detections, a significant performance improvement can be obtained vs. a pure monostatic system.

The paper is organized as follows. After a general introduction in section 1, the measurement setup and the environment are then described in Section 2. The measurement results and their analysis are subsequently discussed in sections 3 and 4. In section 5, a statistical study intended to examine the impact of the RFID reader patterns and the various components of the multistatic system on the BS channel within the UWB range to see how they contribute to improve the performance of the RFID systems. Finally, a conclusion summarizes the work and addresses the main outcomes and perspectives.

2. Measurement techniques and measurement scenarios

In this section, we compare the basic principles and the different methods for the measurement of modulated backscattering. Subsequently, the UWB BS channel measurement scenarios are shown. To check that the BS measurement setup was operating properly, a metallic beer can is employed as the calibration target.

2.1. Transmission and backscattering measurement between the reader and the tag

The measuring principle is depicted in Fig. 2, where the reader sends a signal into the air, which is received by the tag antenna (see Fig. 2) and defined by the S-matrix between the reader antenna (the source feeding) and the tag antenna and backscattered, depending on the status of the load impedance Z_L. Theoretically, the reader/tag system can be described as a

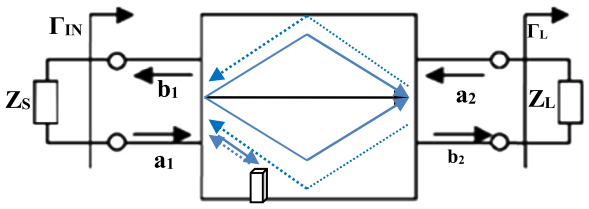

Fig. 2. Measurement and detection principle in the case of multipath propagation, seen as a quadrupole.

linear quadrupole connected to the load. The relationship between the reflected, incident waves and the S-parameter matrix is given by:

$$\begin{bmatrix} b_1 \\ b_2 \end{bmatrix} = \begin{bmatrix} S_{11} & S_{12} \\ S_{21} & S\_22 \end{bmatrix} \begin{bmatrix} a_1 \\ a_2 \end{bmatrix} \tag{1}$$

where a_1 and b_1 are, respectively, the transmitted and received complex wave amplitude by the reader antenna. In the general case, for an imperfectly matched reader antenna, b_1 is the sum of the reflected signal from the reader antenna and of the signal backscattered by the tag antenna and the clutter. In addition, the signal backscattered by the tag antenna is divided into two parts [7]: the first one, which is called "structural mode", is a function of the tag antenna's shape and of the material, whereas the second, called "antenna mode", is a function of the tag antenna load (it carries the useful signal). The parameter $S_{11} = \frac{b_1}{a_1}\Big|_{\text{match}}$ ($Z_L = 50\Omega$) includes the reader antenna reflection, the tag structural mode, and the clutter signal. S_{22} and S_{12} represent the tag reflection coefficient and the transmission coefficient between the reader and the tag at the antenna connector ports. a_2 represents the wave reflected by the load Z_L, which verifies $a_2 = \Gamma_L b_2$, where Γ_L is the reflection coefficient of the tag load. In practice, the measurements were conducted with a vector network analyzer (VNA), which has an excellent dynamic range for accurate measurements. In true MBS measurements, only the port 1 of the VNA was connected to the reader antenna in order to measure the true full backscattered signal between the tag antenna and the reader. Three different tag load conditions have been used: open circuit ($Z_L = \infty$), short circuit ($Z_L = 0$) and matched circuit ($Z_L = Z_C = 50\Omega$). As a result, the antenna mode can be isolated from the structural mode and the clutter signal from the load modulation since, when the tag antenna is loaded with the reference impedance $Z_L = Z_c = 50\Omega$, there is no wave reflected by the load; only the structural part and the clutter signal are backscattered. Thus the useful backscattering signal is derived after time domain processing of the difference between the two measured backscattering responses, when the tag is connected alternatively to the short/open circuit load and to the matched circuit, as:

$$\Gamma_{\text{ant-mode}}(f) = \frac{b_1(f)}{a_1(f)}\bigg|_{\text{load}} - \frac{b_1(f)}{a_1(f)}\bigg|_{\text{match}} \tag{2}$$

However, for enhanced detection range, a variant of the true system has been used, where the load Z_L is replaced by the port 2 of the VNA and the port 1 is connected to the reader antenna. In this way, only the transmission between the antenna ports is measured (one-way channel). However, it is extremely simple to synthesize a full modulated backscattering operation with any load, since the radio channel is reciprocal. Then, by using transmission measurements, the backscattered signal can be expressed as:

$$\Gamma_{\text{ant-mode}}(f) = \frac{\Gamma_L}{1 - \Gamma_L S_{22}(f)} S_{12}(f)\, S_{21}(f) \tag{3}$$

Therefore if the tag antenna is matched with $S_{22} = 0$, the antenna mode of the short-circuit load ($\Gamma_L = -1$) is the opposite of the antenna mode of the open load ($\Gamma_L = +1$). Usually, the two loads are open and short, giving the largest difference.

In Fig. 3, we show the true backscattered signal in the time domain using Eq. (2), for two different tag positions. It can be seen that when the load is changed from open to short, the backscattered signal is basically transformed in its opposite, which supports the proper operation of the modulated backscattering principle. It is also interesting to notice that the pulse amplitude depends on the considered reader-tag direction, according to the tag backscattering radiation and reader antenna radiation properties.

In Fig. 4, we compare the true BS signal (IR_{Bs}) with the BS signal reconstructed from transmission measurements (IR_{TX}), using equation (3) both for the LOS signal and for multipath signals. The horizontal axis represent the round trip time of flight. The relative error between the curves is evaluated using the following error function:

$$\text{Error} = \frac{\int_{\tau_{LOS}}^{\tau_{max}} |IR_{BS}(t) - IR_{TX}(t)|^2 \, dt}{\int_{\tau_{LOS}}^{\tau_{max}} |IR_{BS}(t)|^2 \, dt} \tag{4}$$

where τ_{LOS} represents the delay corresponding to the direct LOS path and τ_{max} represents the last significant delay. The relative error between curves is smaller than (13%). The small difference between the curves is attributed to uncertainties

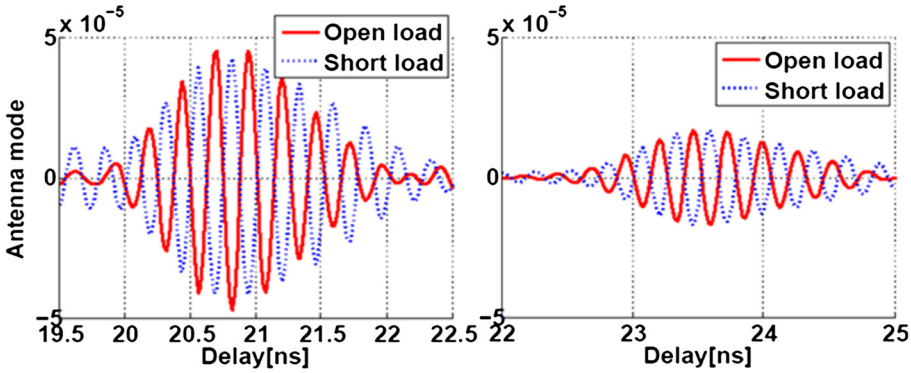

Fig. 3. Example of BS signal for open and short circuits for two different tag positions.

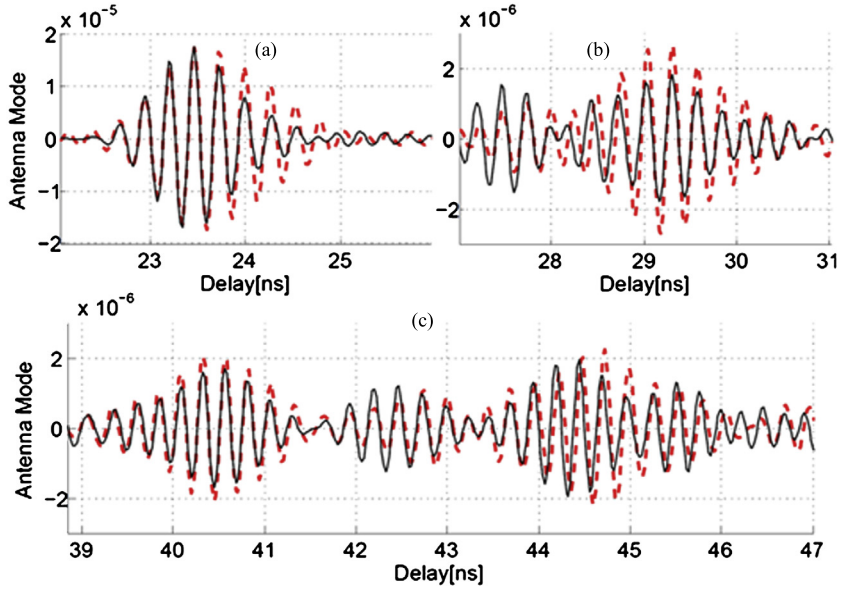

Fig. 4. Comparison between the true measured signal backscattered for open-load impedance (dashed line) and that reconstructed from the transmission measurement (solid line). The direct LoS component: (a) and scattered multipath components in different time windows: (b) and (c).

in clutter signal elimination. Indeed, assuming that the clutter is stationary, the antenna mode using the true MBS measurement method is obtained by subtracting the BS response when the tag is connected alternatively to the short/open circuit load from that obtained when the tag is matched. Owing to manipulations of cables and other channel instabilities over the time lapse necessary for three measurements with three load conditions, it is in practice impossible to perfectly de-embed the clutter response using a true MBS measurement method (in other words, the channel is not purely static).

In conclusion, although the reconstructed response measured is not strictly identical to the true measured BS response, the transmission based method has distinct advantages, being faster with less cable manipulations, and above all providing a much higher dynamic range (i.e. tag measurement distance) because the path loss is twice smaller in dB. This allows more reliable measurements over larger areas.

2.2. Measurements setup

The UWB backscattering channel measurement campaign has been carried out in the 2–6 GHz range, but the processing has been done in the 3–5 GHz range, windowed for Fourier transformation, resulting in an effective band width slightly higher than 1 GHz. This low UWB band (3–5 GHz) has been adopted because of the availability of dedicated hardware. It can be shown that the power gain between the reader antenna input port and the reader antenna output port (identical usually) writes:

$$G(f) = \frac{1}{d^4}\left(\frac{\lambda}{4\pi}\right)^4 \left|H^{\mathrm{T}}_{\mathrm{read}}(f)\right|^4 \left|H^{\mathrm{B}}_{\mathrm{tag}}(f)\right|^2 \tag{5}$$

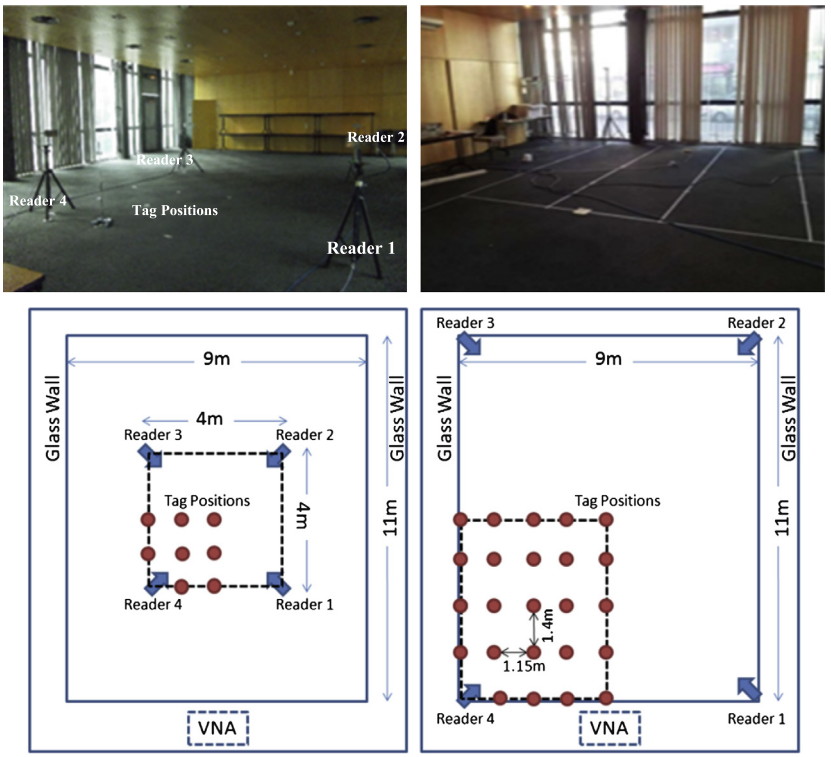

Fig. 5. Scenario; top: room; bottom: small (left) and large (right) scenario.

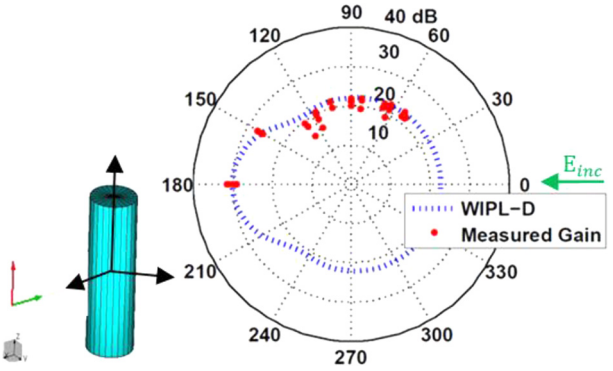

Fig. 6. Comparison between the measured and the computed backscattering gain for a metallic can.

where λ is the wavelength, f the frequency, d the distance, $H^{\mathrm{T}}_{\mathrm{read}}(\mathrm{f})$ is the reader antenna transfer function and $H^{\mathrm{B}}_{\mathrm{tag}}(\mathrm{f})$ is the tag backscattering transfer function. It can also be written in the form $H^{\mathrm{B}}_{\mathrm{tag}}(f) = \frac{4\pi}{\lambda^2}\sigma(f)$, where σ is the scattering cross-section. Since the system measures the difference between two modulated states of the load, the actual system operation can be shown to provide a backscattered signal proportional to the difference of $\frac{\Gamma_{\mathrm{L}}}{1-\Gamma_{\mathrm{L}}S_{22}(\mathrm{f})}$ calculated for the reflection coefficient Γ_{L} of the two loads.

The scenario was a large empty room at the center of which were placed the four reader antennas. The small scenario was used for calibration and the large one for attenuation measurements (Fig. 5).

From Eq. (5), it is possible to verify the good operation of the measuring system by comparing the extracted backscattering gain and the theoretical one for a known object. This was done by using a commercial can of beer, which can be modeled as a closed metallic cylinder and for which the scattering cross-section can be obtained from a commercial full-wave electromagnetic simulator (WIPL-D [8]). As can be seen (Fig. 6 and Fig. 7), the agreement is quite satisfactory. The tags used in the subsequent measurements were either a dual-feed monopole stripline (DFMS, [9]) or a dual-feed monopole microstrip (DFMM, [10]), which are planar-type antennas of size compatible with a tag. The reader antennas were either bicones (omnidirectional, low gain) or Vivaldi (directional, with gain). It is important to recognize that the reader antenna gain is involved twice in the backscattering operation link budget.

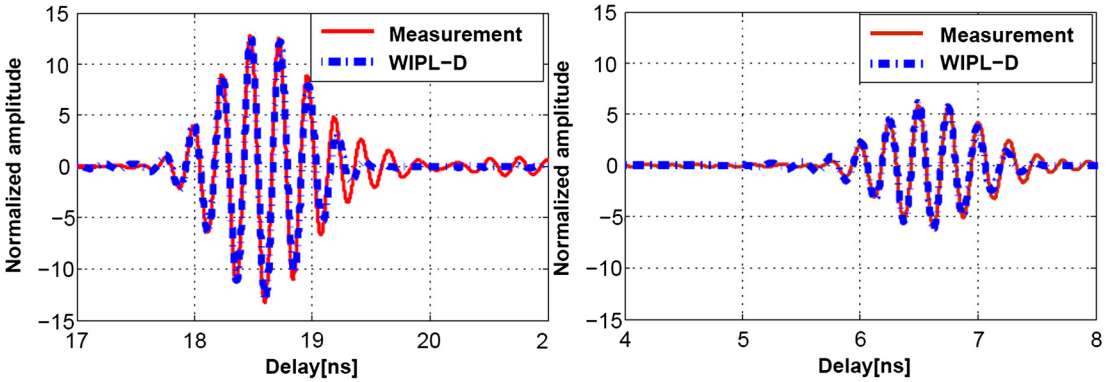

Fig. 7. Can backscattering impulse response for two different direction from the reader antenna to the metallic can. The simulated IR was synchronized with the measurement.

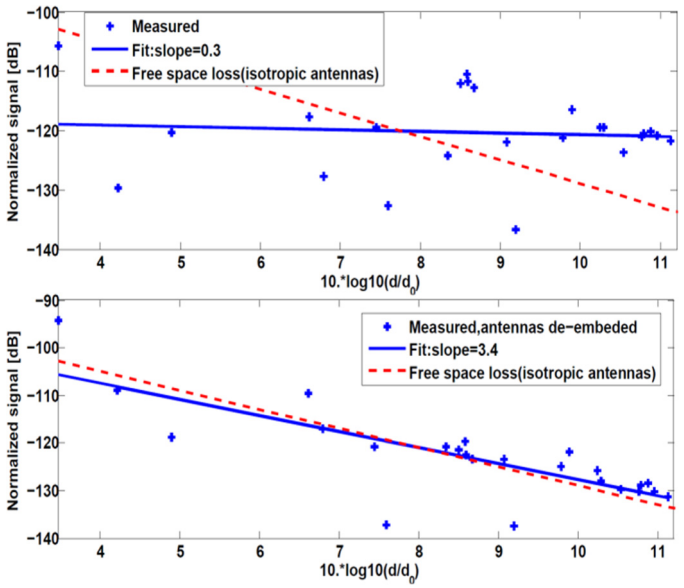

Fig. 8. Gain for the DFMS tag; reader Vivaldi antenna gain included (top) and removed (bottom).

3. Attenuation measurement results

In Fig. 8 and Fig. 9 are shown the backscattered signal for the Vivaldi and the bicone reader antennas, respectively. The antenna gains are included in Fig. 8 (top) and Fig. 9 (top). In Fig. 8 (bottom) and Fig. 9 (bottom), we have removed both reader and tag antenna gains. It can be seen that in the former case, the Friis equation underneath Eq. (5) does not seem respected, from comparing the distance dependence with the expected slope of the 4th power. In the latter case, on the other hand, there is a much better agreement with the theoretical signal, assuming isotropic gainless antennas. The explanation lies in the fact that for a non-isotropic antenna, the signal effectively depends on the precise direction from the reader antenna to the tag, which changes with the tag location (see Fig. 5), both in azimuth and in elevation (when the tag and the reader are not in the same plane).

4. Signal-to-clutter ratio

It is well known that radar systems detection performance is in a good part limited by the clutter backscattered signal, which is often much more important than the target signal. This can be easily understood, in that the cross section of the whole environment (objects but also walls, ground…) is vastly larger than that of a small tag. Thus strategies are necessary to counter these order of magnitude differences. However, designing and optimizing such techniques (basically here, the modulated backscattering principle is assumed to remove a large part of the clutter, which is not modulated) requires a preliminary evaluation of the "signal-to-clutter" (SCR) ratio. This has been done in the scenario described in the previous section, where the clutter can be easily obtained from the VNA measurements through the reflection coefficient at the reader

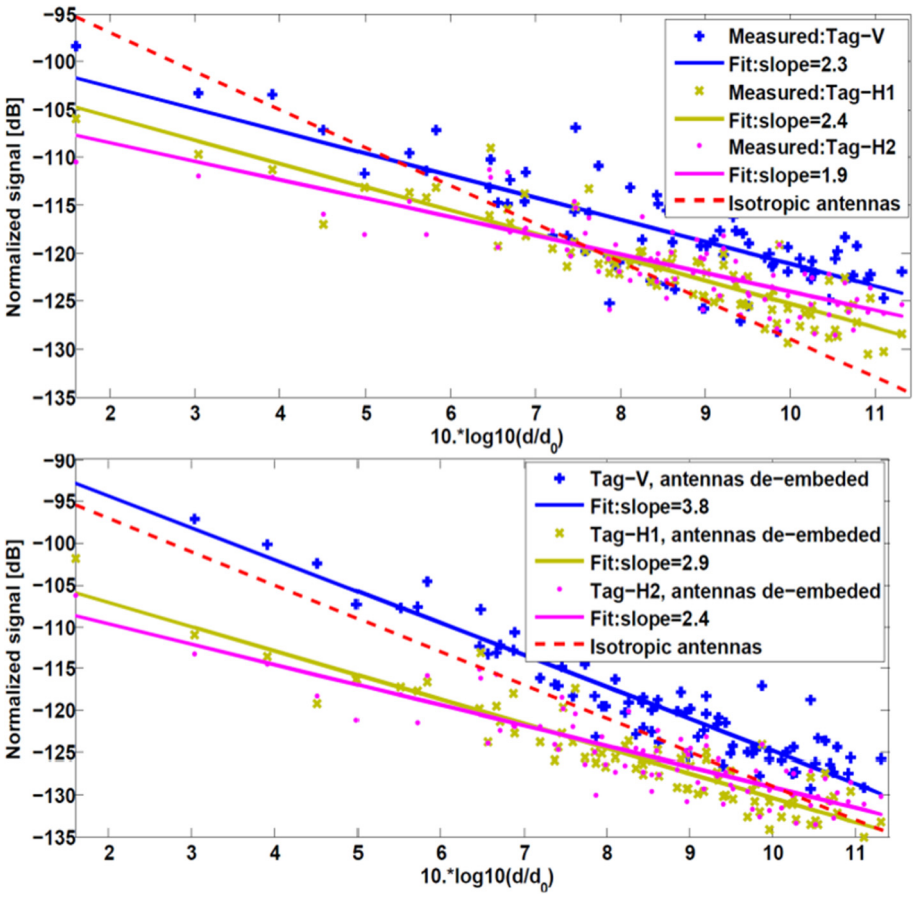

Fig. 9. Gain for the DFMS tag; reader bicone antenna gain included (top) and removed (bottom).

antenna port. This coefficient mainly includes the imperfect matching of the antenna, but it also incorporates the clutter backscattered signal. It is easy to discriminate between both, as the antenna reflection occurs in the very first nanoseconds, while the clutter is found tens of nanoseconds later. The discrimination can be operated after a Fourier transformation to go from the frequency to the time domain.

However, the evaluation of the SCR first needs to clarify its definition. Indeed, for a time-domain based detection system, it may seem appropriate to compute the clutter power and the tag power in the same temporal window (2 ns in practice). This is correct in order to appreciate the needed dynamic range of the analog-to-digital conversion, required to carry out the clutter rejection. However, owing to non-linearities and other saturation effects, the clutter signal over the whole temporal response is important since it might impact the receiver detection capability. Therefore, the SCR involving the whole clutter power has also been used.

The results are shown in Fig. 10 and Fig. 11. It can be seen that the SCR is quite low, especially when comparing the effective tag backscattered signal in the 2-ns time window to the total integrated clutter power. These numbers (~ -50 dB and ~ -60 dB) are valid for the empty environment of the room scenario used, and are expected to be even worse in a more realistic case with more obstructions and objects; this places a hard challenge for the RTLS system design.

5. RFID system performance improvement

In this section, we develop a statistical study intended to examine the impact of the RFID reader patterns and the various components of the multistatic system on the BS channel within the UWB range to see how they contribute to improve the performance of RFID systems.

5.1. Reader antenna pattern optimization

The results of section 3 show that the antenna gain/patterns and the tag antenna orientation have a strong influence on the useful antenna mode signal, with path loss exponents much lower than expected in the case of reader antennas with some directionality. Here we analyze the influence of different reader antenna beams to the BS antenna mode signal.

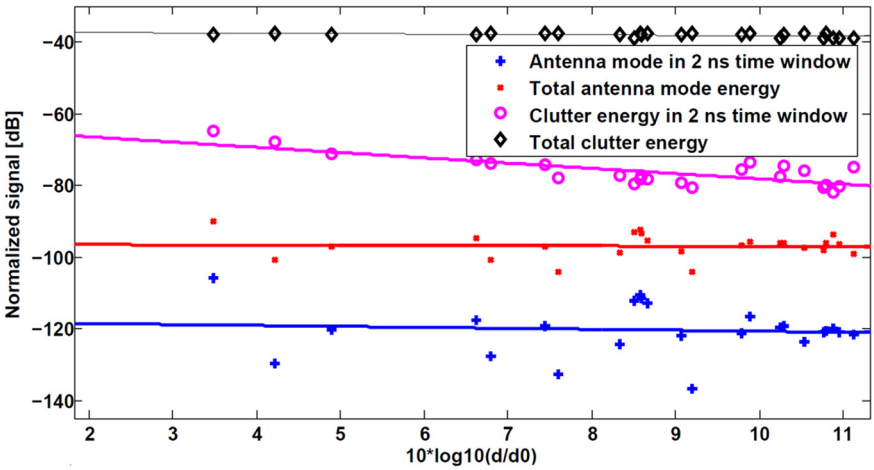

Fig. 10. Relative magnitude of DFMS tag BS energy and clutter energy for the Vivaldi reader antenna.

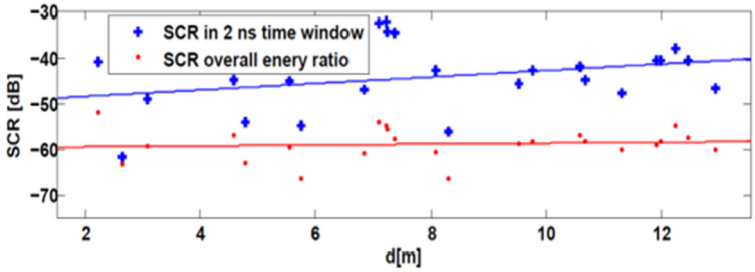

Fig. 11. SCR versus reader-tag separation (Vivaldi reader antenna).

In all practical cases, a reader antenna is located at the higher corner of some region, so it is intuitive to concentrate its radiated power along the directions in which tags are found. This analysis is carried out with the help of synthetic radiation patterns in a pure horizontal plane. We compute the BS antenna mode signal considering that the tag is enclosed inside a constellation of four identical reader antennas located at the four corners of a rectangle of $11 \times 9\text{m}^2$. The normalized reader antenna power pattern for high and low directivity is approximated by a cosine function raised to a power m [11]:

$$G_m = D_{\max} (\cos\theta)^m \tag{6}$$

where θ is the angle with respect to antenna boresight, m is chosen to define the antenna beamwidth, and $D_{\max}$ is the peak directivity, which is also a function of m. Using the Friis equation, the BS tag power received at the reader antenna decreases with the distance according to an exponent factor of 4. It is also proportional to the square of the reader antenna gain.

Owing to the directionality of the reader (for a given m value), the linear regression of the round trip path gain versus the logarithm of the reader tag distance is shown in Fig. 12 (left), and the cumulative distribution function (CDF) is computed also to show the statistic of the deviation of the antenna mode around the mean Fig. 12 (right).

What comes out of these graphs is the following:

- the path loss exponent decreases with the directivity, but the spread of the BS signal around the linear regression increases;
- if a too high directivity is chosen, the BS gain improves slightly for specific directions, but this always comes at the cost of much worse BS gain in other directions, as the size of the beam is inversely proportional to the directivity gain. Then we have reduced the ability to see tags outsides the main beam;
- with a moderately directional antenna (large beam width), the result ought to be an increase in the read range comparing with an isotropic antenna ($m = 0$). This is depicted graphically in Fig. 12 (left) for an antenna with $m = 5$. For example, for a normalized sensitivity of -110 dB, the read range increases approximately by 3m relative to that obtained with an isotropic reader antenna.

We see indeed that the reader antenna beam width plays a very large role in the achievable read range. Using highly directional antenna should, therefore, be avoided. Given the reader sensitivity, the power of the signal transmitted by the

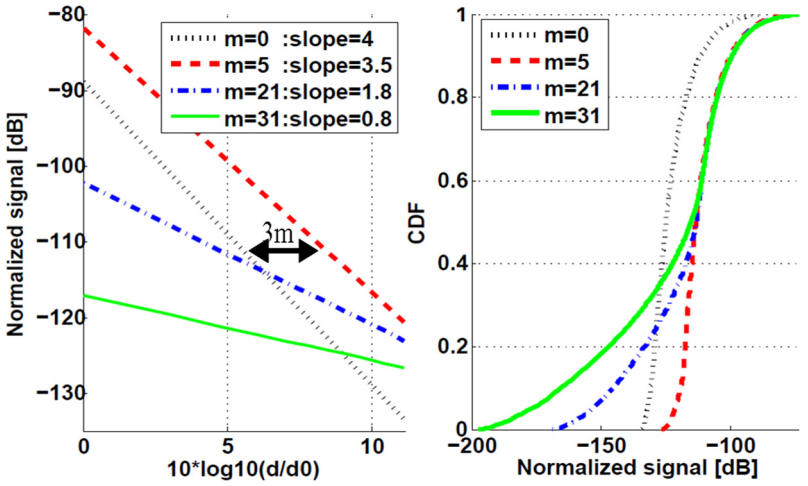

Fig. 12. Antenna mode for different reader antenna directionality.

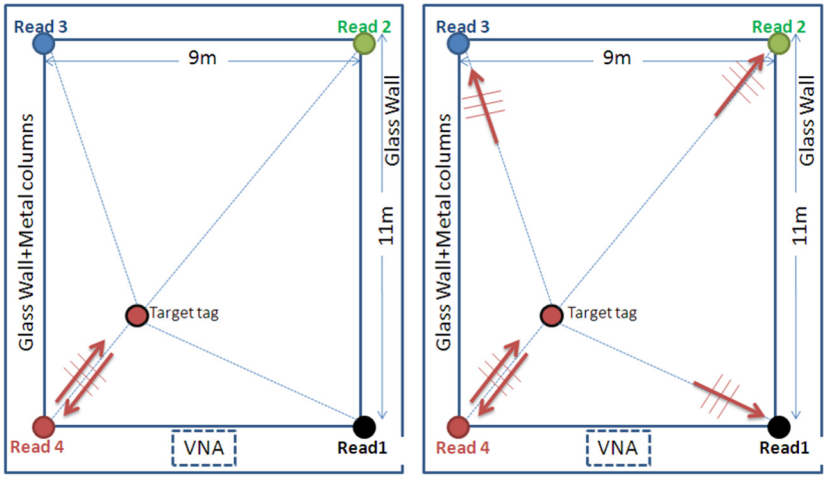

Fig. 13. Operation modes: Monostatic (left) vs. multistatic. Right: when reader 4 transmits.

reader, and by taking into account a margin of 20 dB reduced due to the masking effects by the tagged object, an appropriate optimization of the reader antenna directivity may then significantly improve the overall system performance.

5.2. Monostatic vs. bistatic operation

To compute unambiguously the location of the tag, at least three "anchors" with known positions are required. Therefore, by using the position information provided by three readers, the system can draw three circles where the radius are the measured distances (ranging) and the centers are the known reader positions [12,13]. The reader operating principle (monostatic or bistatic configuration) is driven by tradeoffs in cost and performance. The vast majority of RFID applications operate in monostatic mode, using a single antenna for transmission and reception. This is due to their relative simplicity to deploy. However, bistatic detection maximizes the isolation between the transmitter and the receiver, making tag useful signal detection easier. Multistatic operation uses the two basic reader configurations (monostatic and bistatic). All reader nodes in this network can operate as transmitters, receivers or both transmitters and receivers. The discrimination between tag and reader signals is carried out in the time domain and also based on codes. The reader antenna can remotely detect and identify a tag, provided the measured LOS backscattered power P_{BS} exceeds a certain threshold.

Based on these considerations, we develop in this part a statistical study intended to compare the minimum bound of the received backscattered power, in two different modes of operations (Fig. 13):

1) mode 1: this is the traditional monostatic detection, where each reader is transmitting a specific waveform and is detecting only the BS signal originating from this waveform. The four readers are independent and provide their own ranging and identification data;

2) mode 2: both bistatic and monostatic configurations are used. When an (active) reader transmits, it carries out monostatic tag MBS detection, while the other (passive) readers act only as receivers and collect the scattered signals by this same

tag. This mode introduces additional complications (such as synchronization), but it is expected to improve the detection and thus localization performance.

In the following, the tag parameters (location, characteristics) are taken as random variables within the 2D rectangular area enclosed by the four readers, which allows one to compute a statistical distribution of the best received signal and compare between the detection modes. We carried out the following computations of the required BS received power for the detection. Let k be a tag position of the entire set of measured channel realizations R and $P_{mn}(k)$ the backscattered tag power delivered into the reader receiver n originating from the reader transmitter m. Then we computed the mode 1 and mode 2 BS powers $P^j_{\mathrm{BS1}}(k)$ and $P^j_{\mathrm{BS2}}(k)$, where the superscript j denotes the number of reader antennas required for tag detection: 1 means that a single tag detection is required, 2: at least 2 readers must be able to detect etc. Thus in mode 1 we have:

$$\begin{cases} P^1_{\mathrm{BS1}}(k) = \mathrm{Max}_m \{P_{mm}(k)\} \\ P^4_{\mathrm{BS1}}(k) = \mathrm{Min} \{P_{mm}(k)\} \end{cases} \tag{7}$$

The intermediate cases are more complicated to write, e.g., $P^2_{BS1}(k) = \mathrm{Max}_{m \neq M(k)} \{P_{mm}(k)\}$ with $M(k) = Arg P^1_{BS1}(k)$. In mode 2, we have, for instance:

$$\begin{cases} P^1_{\mathrm{BS2}}(k) = \mathrm{Max}_{m,n} \{P_{mn}(k)\} \\ P^4_{\mathrm{BS2}}(k) = \mathrm{Min}_m [\mathrm{Max}_n \{P_{mn}(k)\}] \end{cases} \tag{8}$$

and related expressions for the intermediate cases of two or three detecting readers.

In all results presented below, the computed BS powers are normalized by the transmitted reader power, and integrated over a 2-ns duration of the LOS signal. Since the tag position is random, the observed relative backscattering power P^j_{BS} is random as well and considered to be a random variable X with a probability-density function (PDF) $f_X(x)$. Let K be the two- or three-dimensional random variable representing the tag position, with PDF $f_K(k)$. Using the law of total probability, $f_X(x)$ is expressed as:

$$f_X(x) = \int f_{X/K}(x \mid k)\, f_K(k)\, \mathrm{d}k \tag{9}$$

Equation (5) can be easily reused for the bistatic case in single path LOS propagation, where both reader antenna transfer functions enter the received BS signal in the proper transmitting and receiving directions, and the tag transfer function is similarly involved twice:

$$G_{mn} = \left(\frac{\lambda}{4\pi}\right)^4 \cdot \left(\frac{1}{r_n}\right)^2 \cdot \left(\frac{1}{r_m}\right)^2 \cdot \left|H^{T_m}_{\mathrm{read}}\left(f, \Omega^{\mathrm{read}}_{\mathrm{inc}_m}\right)\right|^2 \cdot \left|H^{T_n}_{\mathrm{read}}\left(f, \Omega^{\mathrm{read}}_{\mathrm{sc}_n}\right)\right|^2 \left|H^{B}_{\mathrm{tag}}\left(f, Z_L, \Omega^{\mathrm{tag}}_{\mathrm{inc}_m}, \Omega^{\mathrm{tag}}_{\mathrm{Sc}_n}\right)\right|^2 \tag{10}$$

where m and n refer to the transmitting and receiving reader antenna, respectively. Then we have $X = P_t G_{mn}$, with P_t the transmitted power by any reader.

In the general case, $H^{\mathrm{B}}_{\mathrm{tag}}$ is a random variable, owing to the intrinsic tag antenna variability and, even more, to the strong influence of the objects on which tags are placed [14,15]. If we assume that the tag location is independent from its characteristics and from those of the objects, this result in the factorization:

$$f_{X/K}(x \mid k) = f_{X/K}\big(y(k) \cdot z \mid k\big) = f_{X/K}\big(y(k) \cdot z\big) = \frac{1}{y(k)} f_Z\left(\frac{x}{y(k)}\right) \tag{11}$$

where $y(k) = P_t \left|\frac{\lambda^2 H^{T_m}_{\mathrm{read}} H^{T_n}_{\mathrm{read}}}{16\pi^2 r_m \cdot r_n}\right|^2$ denotes the pure propagation and reader antenna part of the received power, which is a fully deterministic function of the tag location and $z = \left|H^{\mathrm{B}}_{\mathrm{tag}}\right|^2$, of probability density $f_Z(z)$. Then:

$$f_X(x) = \int \frac{1}{y(k)} f_Z\left(\frac{x}{y(k)}\right) f_K(k)\, \mathrm{d}k \tag{12}$$

In the following, we restrict to a pure hypothetical tag, for which $\left|H^{\mathrm{B}}_{\mathrm{tag}}\right|^2 = 1$. Thus we have a pure Dirac distribution $f_Z(z) = \delta(z-1)$ and:

$$f_X(x) = \int \frac{1}{y(k)} \delta\left(\frac{x}{y(k)} - 1\right) f_K(k)\, \mathrm{d}k = \int \delta\big(x - y(k)\big) f_K(k)\, \mathrm{d}k \tag{13}$$

We finally obtain the CDF function of the backscattered tag power:

$$F_X(x) = \int_0^x f_X(u)\, \mathrm{d}u = \int H_{\mathrm{V}}\big(x - y(k)\big) f_K(k)\, \mathrm{d}k \tag{14}$$

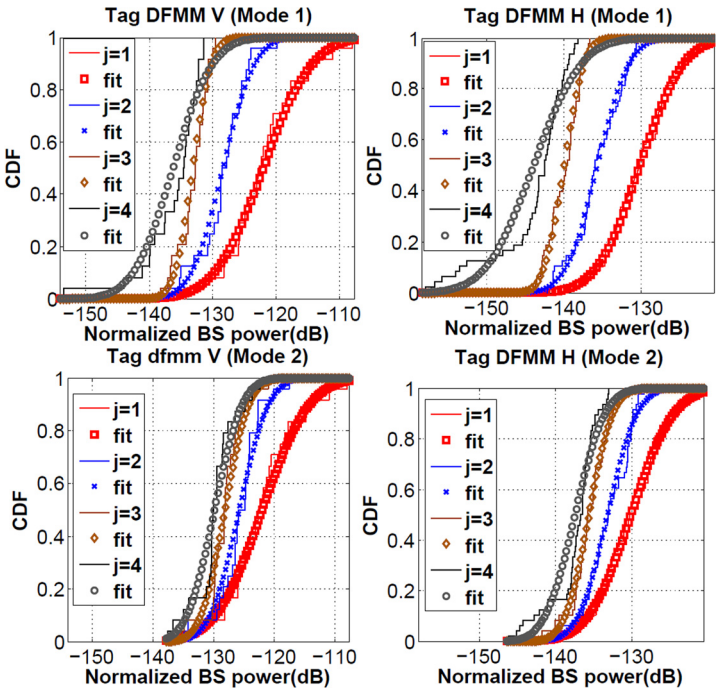

Fig. 14. The statistical distribution of the BS tag power seen by a vertical bicone reader.

where H_V is the Heaviside step function. This formula has a very simple geometric interpretation: for a uniform spatial distribution of tag positions, $F_X(x)$ is nothing else than the proportion of positions for which the received power exceeds x.

The advantage of this probabilistic formulation is that it can be easily generalized, through Eq. (12) and the choice of a suitable distribution for $f_Z\left(\left|H_{\text{tag}}^{\text{B}}\right|^2\right)$, in order to express high tag and objects variability, according to the results of [14,15]. However, we here restrict ourselves to the hypothetical isotropic scattering tag, in order to evaluate the basic performance improvement brought by multistatic detection.

The measurement campaign has been carried out in a large room (see Fig. 13) over the 2–6-GHz band, but the processing has been done in the 3–5-GHz band, windowed for Fourier transformation, resulting in an effective band width slightly higher than 1 GHz. The tag used was a DFMM, which is a planar-type antenna of size compatible with a tag. From Eq. (14), the CDF of $P_{\text{BS1,2}}^{j}(k)_{K\in\mathcal{R}}$ for the two operation modes explained above are easily computed and are shown in Fig. 14. The curves are fitted with the normal distribution (in dB, i.e. lognormal) using the parameters listed in Table 1, in the case where the tag is either vertically V or horizontally H oriented.

Some simple conclusions can be drawn from these results: when the reader antenna operates according to the first mode (monostatic), the limiting received BS power is about lower by 14 dB for a single reader detection (no localization) than for all four readers detection (accurate localization). When the reader antennas operate according to the second mode (multistatic), we find 7.8 dB instead. In other words, full localization requires only a 7.8-dB better reader's sensitivity, while a 14-dB better sensitivity is required for mode 1. This improvement can be understood as macrodiversity, since for a given tag position, 16 signals are used instead of four. The other interesting result is that mode-2 operation provides on average a 6.4-dB improvement for accurate localization with respect to mode 1. Although the numbers above are for vertical polarization, they do not much differ for horizontal polarization.

Finally, what is clear from looking at Fig. 14 and Table 1 is that mode-2 operation not only improves the mean BS powers, but also reduces the spread. This is another very attractive feature of the diversity effect inherent to the multistatic approach.

6. Conclusion

In the present work, we have conducted a study on the backscattering channel for a RTLS system of ultra wide band tags and readers [16]. There are many challenges that derive from the 4th power dependence of the tag backscattered signal and from the low transmission power enforced by regulations. We found that this fourth power is not generally verified, because of directional antenna effects from the reader antenna, and also because the signal-to-clutter ratio was very small, even for the empty character of the room used in measurements. The design and optimization of such a system needs to take into account these effects in the evaluation of its coverage in practical cases.

Table 1
Fitted Gaussian distribution parameter estimates for tag BS power seen by a vertical bicone reader.

j	Tag vertically oriented			
	Mode 1		Mode 2	
	Mean	Std	Mean	Std
1	−122.0	6.0	−122.0	6.0
2	−128.3	3.9	−125.7	3.7
3	−133.1	2.3	−128.1	3.1
4	−136.2	4.9	−129.8	3.5
j	Tag horizontally oriented			
	Mode 1		Mode 2	
	Mean	Std	Mean	Std
1	−130.1	4.3	−130.1	4.3
2	−135.7	3.2	−133.2	3.0
3	−140.0	2.0	−135.6	2.4
4	−143.9	4.8	−137.4	3.0

We also showed that, by considering multistatic scattering based on both monostatic and bistatic detection, a significant performance improvement can be obtained vs. a pure monostatic system, owing to macro-diversity.

In this work, only reference tag antennas have been considered, with omnidirectional antenna patterns. However, an even bigger degradation is expected in a large angular sector when the tag is placed on an object, which is the main use of RFID tag [15]. The statistical method developed here (Eqs. (11)–(14)) lends itself easily to a generalization taking into account the dramatic variability in the backscattering gain for tags placed on objects [14], which can be expressed through a monostatic or bistatic model of this gain. This will be the subject of a future work.

Acknowledgements

The research leading to these results has received funding from the European Union Seventh Framework Programme FP7/2007-2013 under grant agreement No. 257544.

References

[1] R. D'Errico, M. Bottazzi, F. Natali, E. Savioli, S. Bartoletti, A. Conti, D. Dardari, N. Decarli, F. Guidi, F. Dehmas, L. Ouvry, U. Alvarado, N. Hadaschik, C. Frankek, Z. Mhanna, M. Sacko, Y. Wei, A. Sibille, An UWB-UHF semi-passive RFID system for localization and tracking applications, in: IEEE RFID TA, Nice, France, November 2012, pp. 5–7.
[2] D. Pech, et al., Ultrahigh-power micrometer-sized supercapacitors based on onion-like carbon, Nat. Nanotechnol. Lett. 5 (2010) 651.
[3] Y. Shen, C. Law, A low-cost UWB-RFID system utilizing compact circularly polarized chipless tags, IEEE Antennas Wirel. Propag. Lett. 11 (2012) 1382–1385.
[4] S. Hu, Y. Zhou, C. Law, W. Dou, Study of a uniplanar monopole antenna for passive chipless UWB-RFID localization system, IEEE Trans. Antennas Propag. 58 (2) (2010) 271–278.
[5] M.A. Morgan, Ultra-wideband impulse scattering measurements, IEEE Trans. Antennas Propag. 42 (1994) 840–846.
[6] A. Molisch, D. Cassioli, C.C. Chong, S. Emami, A. Fort, B. Kannan, J. Kåredal, J. Kunisch, H.G. Schantz, K. Siwiak, M.Z. Win, A comprehensive standardized model for ultrawideband propagation channels, IEEE Trans. Antennas Propag. 54 (11) (2006) 3151–3166.
[7] R. Hansen, Relationships between antennas as scatterers and as radiators, Proc. IEEE 77 (5) (1989) 659–662.
[8] See http://www.wipl-d.com/.
[9] S. Bories, H. Ghannoum, C. Roblin, Robust planar stripline monopole for UWB terminal applications, in: Proc. 2005 IEEE International Conference on UltraWideband, 2005.
[10] H. Ghannoum, S. Bories, R. D'Errico, Small-size UWB Planar antenna and its behaviour in WBAN/WPAN applications, in: Seminar on Ultra Wideband Systems, Technologies and Applications, 2006, The Institution of Engineering and Technology, 2006, pp. 221–225.
[11] C. Balanis, Antenna Theory, 3rd ed., Wiley, 2005.
[12] E. Paolini, A. Giorgetti, M. Chiani, R. Minutolo, M. Montanari, Localization capability of cooperative anti-intruder radar systems, EURASIP J. Adv. Signal Process. (2008) (special issue on cooperative localization in wireless ad hoc and sensor networks).
[13] H. Karl, A. Willig, Protocols and Architectures for Wireless Sensor Networks, Wiley, Chichester, UK, 2006.
[14] A. Sibille, M. Sacko, Z. Mhanna, F. Guidi, C. Roblin, Joint antenna-channel statistical modelling of UWB backscattering RFID, in: ICUWB, Bologna, Italy, September 2011, pp. 14–16.
[15] F. Guidi, A. Sibille, C. Roblin, V. Casadei, D. Dardari, Analysis of UWB tag backscattering and its impact on the detection coverage, IEEE Trans. Antennas Propag. 62 (8) (2014) 4292–4303.
[16] http://www.selectwireless.eu.